DYNAMIC THEORY OF THE RELATIVISTIC ELECTRON RADIATION IN PERIODIC LAYERED MEDIUM IN LAUE GEOMETRY

S.V. Blazhevich[1], Ju.P. Gladkih[1], A.V. Noskov[2*]

[1] *National Research University Belgorod State University, 308015, Belgorod, Russia;*

[2] *Belgorod University of Cooperation, Economics and Low, 308023, Belgorod, Russia*

(Received May 11, 2012)

A theory of coherent X-ray radiation of a relativistic electron crossing the artificial periodic medium in the Laue scattering geometry is constructed. The expressions describing the spectral and angular characteristics of radiation in the direction of Bragg scattering are obtained and investigated. By analogy with the radiation emission in a crystalline medium this radiation is considered as the result of coherent summation of the contributions of two radiation mechanisms: parametric (PXR) and diffracted transition (DTR). It is shown that the yield of DTR from layered target can be more than one order higher than the yield in single crystal radiator, under similar conditions. The manifestations of the Borrmann effect for DTR in the artificial multilayer environment are demonstrated for a Laue scattering geometry.

PACS:78.70.-g; 78.70.Ck; 79.90.tt

1. INTRODUCTION

When a charged particle crosses the entrance surface of the crystal plate the transition radiation arises (TR) [1], which then is diffracted by a system of parallel atomic planes of the crystal, forming the diffracted transition radiation DTR [2-4]. At the same time a charged particle Coulomb field is scattered by a system of parallel atomic planes of the crystal, creating a parametric X-ray radiation (PXR) [5-7]. In the scheme of the symmetric reflection when the system of diffracting atomic planes is perpendicular (in the case of Laue scattering geometry) or parallel (in the case of Bragg scattering) to the surface of the crystal plate, the radiation mechanisms in the two-wave approximation of dynamic diffraction theory were considered in [8-11]. In the general case of asymmetric reflection of the radiation from the plate when the diffracted atomic planes make an arbitrary angle with the surface of the plate, the dynamic effects of PXR and DTR are considered in [12-15], where it was shown that by changing the asymmetry of reflection, we can significantly increase the radiation yield. Traditionally, the radiation of a relativistic particle in a periodically layered structure was considered in the Bragg scattering geometry for the case where the reflecting layers are parallel to the entrance surface, i.e. for the case of symmetric reflection. The radiation in a periodic layered structure is usually viewed as resonant transition radiation [5, 16]. In the works [17], the radiation from an artificial periodic structure was represented as the sum of diffracted transition radiation (DTR) and parametric X-ray radiation (PXR). In the cited works the radiation of relativistic particles in an artificial periodic structure was considered only in the Bragg scattering geometry for the special case of symmetric reflection of the particle field with respect to the target surface, when the diffracted layers are parallel to the target surface. In the present paper we consider the coherent X-ray radiation scattering in the Bragg direction generated by relativistic electron crossing the artificial periodic structure in the Laue scattering geometry. By analogy with the crystalline environment the coherent radiation is considered as the sum of PXR and DTR contributions. On the basis of two-wave approximation of dynamic diffraction theory [18] the expressions describing the spectral and angular characteristics of radiation are derived.

2. AMPLITUDE OF THE RADIATION

We analyze the radiation emitted by a relativistic electron passing through a multilayer structure (Fig. 1) consisting of periodically arranged amorphous layer with thickness a and b respectively (is the structure period) with the dielectric susceptibility χ_a and χ_b respectively.

We consider the equation for the Fourier transform of the electromagnetic field

$$\mathbf{E}(\mathbf{k},\omega) = \int dtd^3\mathbf{r}\mathbf{E}(\mathbf{r},t)\exp(i\omega t - i\mathbf{k}\mathbf{r})\,. \quad (1)$$

We use the two-wave approximation of dynamic diffraction theory, in which the incident and diffracted

*Corresponding author E-mail address: noskovbupk@mail.ru

wave are considered on equal grounds. Since the electromagnetic field associated with a relativistic particle can accurately be considered as transverse both incident $\mathbf{E}_0(\mathbf{k},\omega)$ and diffracted $\mathbf{E}_{\mathbf{g}}(\mathbf{k},\omega)$ electromagnetic waves are determined by two amplitudes with different values of transverse polarization

$$\mathbf{E}_0(\mathbf{k},\omega) = E_0^{(1)}(\mathbf{k},\omega)\mathbf{e}_0^{(1)} + E_0^{(2)}(\mathbf{k},\omega)\mathbf{e}_0^{(2)}\,,$$

$$\mathbf{E}_{\mathbf{g}}(\mathbf{k},\omega) = E_{\mathbf{g}}^{(1)}(\mathbf{k},\omega)\mathbf{e}_1^{(1)} + E_{\mathbf{g}}^{(2)}(\mathbf{k},\omega)\mathbf{e}_1^{(2)}\,, \qquad (2)$$

where the unit vectors of polarization $\mathbf{e}_0^{(1)}$ and $\mathbf{e}_0^{(2)}$ are perpendicular to vector $\mathbf{k}$, and vectors $\mathbf{e}_1^{(1)}$ and $\mathbf{e}_1^{(2)}$ are perpendicular to vector $\mathbf{k}_{\mathbf{g}} = \mathbf{k}+\mathbf{g}$. Vectors $\mathbf{e}_0^{(2)}$ and $\mathbf{e}_1^{(2)}$ lie in the plane of the vectors $\mathbf{k}$ and $\mathbf{k}_{\mathbf{g}}$ (π-polarization), and vectors $\mathbf{e}_0^{(1)}$ and $\mathbf{e}_1^{(1)}$ are perpendicular to this plane (σ-polarization). The vector $\mathbf{g}$ is defined similarly to the reciprocal lattice vector in the crystal - it is perpendicular to the layers of protection, and its length is equal to $\mathbf{g} = \frac{2\pi}{T}n, n = 0, \pm1, \pm2, \cdots$

The equations for the Fourier transform of the electromagnetic field in a two-wave approximation of dynamical diffraction theory have the form [19]:

$$\begin{cases} (\omega^2(1+\chi_0) - k^2)E_0^{(s)} + \omega^2\chi_{-\mathbf{g}}C^{(s)}E_{\mathbf{g}}^{(s)} = 8\pi^2 ie\omega\theta V P^s\delta(\omega - \mathbf{kV}), \\ \omega^2\chi_{\mathbf{g}}C^{(s)}E_0^{(s)} + (\omega^2(1+\chi_0) - k_{\mathbf{g}}^2)E_{\mathbf{g}}^{(s)} = 0, \end{cases} \qquad (3)$$

where $\chi_{\mathbf{g}}$, $\chi_{-\mathbf{g}}$ are coefficients of the Fourier expansion of the periodic structure dielectric susceptibility over the reciprocal vectors $\mathbf{g}$:

$$\chi(\omega,\mathbf{r}) = \sum_{\mathbf{g}}\chi_{\mathbf{g}}(\omega)exp(i\mathbf{gr}) = \sum_{\mathbf{g}}(\chi'_{\mathbf{g}}(\omega) + i\chi''_{\mathbf{g}}(\omega)exp(i\mathbf{gr})\,. \qquad (4)$$

The values C^s and P^s in the system (3) are defined as follows

$$C^{(s)} = \mathbf{e}_0^{(s)}\mathbf{e}_1^{(s)}, C^{(1)} = 1, C^{(2)} = \cos 2\theta_B\,,$$

$$P^{(s)} = \mathbf{e}_0^{(s)}(\mu/\mu), P^{(1)} = \sin\varphi, P^{(2)} = \cos\varphi, \qquad (5)$$

where $\mu = \mathbf{k} - \omega\mathbf{V}/\mathbf{V^2}$ is the component of the virtual photon momentum perpendicular to the particle velocity $\mathbf{V}$, $\mu = \omega\theta/V, \theta \ll 1$ is the angle between vectors $\mathbf{k}$ and V, θ_B is Bragg angle, φ is the radiation azimuth angle measured from the plane formed by the velocity vector $\mathbf{V}$ and $\mathbf{g}$

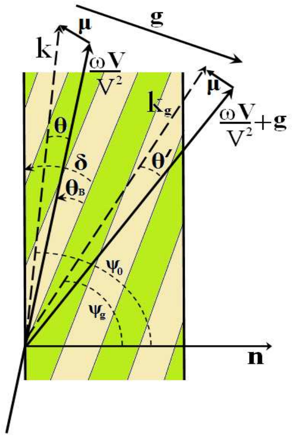

Fig.1. *Geometry of the radiation process and the system of the using parameters notations, θ and θ' are the radiation angles, θ_B is Bragg angle, $\mathbf{k}$ and $\mathbf{k}_g$ are wave vectors of incident and diffracted photons*

The vector $\mathbf{g}$ length can be also expressed through the Bragg angle θ_B and the Bragg frequency ω_B: $g = 2\omega_B\sin\theta_B/V$. The angle between the vector $\frac{\omega\mathbf{V}}{V^2}$ and the wave vector $\mathbf{k}$ of the incident wave is marked θ and the angle between the vector $\frac{\omega\mathbf{V}}{V^2} + \mathbf{g}$ and the diffracted wave vector $\mathbf{k}_{\mathbf{g}}$ is indicated as θ'. The system (3) under $s = 1$ describes the fields of σ-polarization, and under $s = 2$ the fields of π-polarization. The values χ_0 and $\chi_{\mathbf{g}}$ are defined as follows:

$$\chi_0(\omega) = \frac{a}{T}\chi_a + \frac{b}{T}\chi_b,$$

$$\chi_{\mathbf{g}}(\omega) = \frac{exp(-iga) - 1}{igT}(\chi_b - \chi_a)$$

$$\chi'_0 = \frac{a}{T}\chi'_a + \frac{b}{T}\chi'_b, \quad \chi''_0 = \frac{a}{T}\chi''_a + \frac{b}{T}\chi''_b$$

$$Re\sqrt{\chi_{\mathbf{g}}\chi_{-\mathbf{g}}} = \frac{2\sin(\frac{ga}{2})}{gT}(\chi'_b - \chi'_a),$$

$$Im\sqrt{\chi_{\mathbf{g}}\chi_{-\mathbf{g}}} = \frac{2\sin(\frac{ga}{2})}{gT}(\chi''_b - \chi''_a)\,. \qquad (6)$$

By solving the dispersion equation following from the system (3)

$$(\omega^2(1+\chi_0) - k^2)(\omega^2(1+\chi_0) - k_{\mathbf{g}}^2) - \omega^4\chi_{-\mathbf{g}}\chi_{\mathbf{g}}{C^{(s)}}^2 = 0 \qquad (7)$$

with the use of standard methods of dynamical theory [18], we find the expression for k and $k_{\mathbf{g}}$:

$$k = \omega\sqrt{1+\chi_0} + \lambda_0, k_{\mathbf{g}} = \omega\sqrt{1+\chi_0} + \lambda_{\mathbf{g}}, \qquad (8)$$

$$\lambda_{\mathbf{g}}^{(1,2)} = \frac{\omega}{4}(\beta \pm \sqrt{\beta^2 + 4\chi_{\mathbf{g}}\chi_{-\mathbf{g}}{C^{(s)}}^2\frac{\gamma_{\mathbf{g}}}{\gamma_0}}), \qquad (9)$$

$$\lambda_0^{(1,2)} = \omega\frac{\gamma_0}{4\gamma_{\mathbf{g}}}(-\beta \pm \sqrt{\beta^2 + 4\chi_{\mathbf{g}}\chi_{-\mathbf{g}}{C^{(s)}}^2\frac{\gamma_{\mathbf{g}}}{\gamma_0}}), \qquad (10)$$

where $\beta = \alpha - \chi_0(1 - \frac{\gamma_{\mathbf{g}}}{\gamma_0})$, $\alpha = \frac{1}{\omega^2}(k_{\mathbf{g}}^2 - k^2)$, $\gamma_0 = \cos\psi_0$, $\gamma_{\mathbf{g}} = \cos\psi_{\mathbf{g}}$, ψ_0 - the angle between the wave vector of the incident wave $\mathbf{k}$ and vector normal to the surface of the plate $\mathbf{n}$, $\psi_{\mathbf{g}}$ is the angle between the wave vector $\mathbf{k}_{\mathbf{g}}$ and the vector $\mathbf{n}$ (see Figure 1).

Dynamic additions λ_0 and $\lambda_{\mathbf{g}}$ for X-ray wave vectors are related by formula

$$\lambda_{\mathbf{g}} = \frac{\omega\beta}{2} + \lambda_0 \frac{\gamma_{\mathbf{g}}}{\gamma_0}. \tag{11}$$

Since the dynamic additions are small: $|\lambda_0| \ll \omega$, $|\lambda_{\mathbf{g}}| \ll \omega$, one can show that $\theta \approx \theta'$ (see Fig. 1), therefore further we will use the notation for both of these angles.

We represent the solution of the system of equations (3) for the diffracted field in a periodic structure in such a form:

$$E_{\mathbf{g}}^{(s)medium} = -\frac{8\pi^2 ieV\theta P^{(s)}}{\omega} \frac{\omega^2 \chi_{\mathbf{g}} C^{(s)}}{4\frac{\gamma_0^2}{\gamma_{\mathbf{g}}^2}(\lambda_{\mathbf{g}} - \lambda_{\mathbf{g}}^{(1)})(\lambda_{\mathbf{g}} - \lambda_{\mathbf{g}}^{(2)})} \times$$
$$\times \delta(\lambda_{\mathbf{g}} - \lambda_{\mathbf{g}}^*) + E_{\mathbf{g}}^{(s)^{(1)}} \delta(\lambda_{\mathbf{g}} - \lambda_{\mathbf{g}}^{(1)}) + E_{\mathbf{g}}^{(s)^{(2)}} \delta(\lambda_{\mathbf{g}} - \lambda_{\mathbf{g}}^{(2)}), \tag{12a}$$

where $\lambda_0^* = \omega(\frac{\gamma^{-2}+\theta^2-\chi_0}{2})$, $\lambda_{\mathbf{g}}^* = \frac{\omega\beta}{2} + \frac{\gamma_{\mathbf{g}}}{\gamma_0}\lambda_0^*$, $\gamma = 1/\sqrt{1-V^2}$-Lorentz factor of the particle, $E_{\mathbf{g}}^{(s)^{(1)}}$ and $E_{\mathbf{g}}^{(s)^{(2)}}$ are free diffracted fields in the multilayer target. For the field in vacuum in front of the radiator the solution of (3) has the form:

$$E_0^{(s)vacI} = \frac{8\pi^2 ieV\theta P^{(s)}}{\omega} \frac{1}{-\chi_0 - \frac{2}{\omega}\lambda_0} \delta(\lambda_0 - \lambda_0^{(*)}) = \frac{8\pi^2 ieV\theta P^{(s)}}{\omega} \frac{1}{\frac{\gamma_0}{\gamma_{\mathbf{g}}}(-\chi_0 - \frac{2}{\omega}\frac{\gamma_0}{\gamma_{\mathbf{g}}}\lambda_{\mathbf{g}} + \beta\frac{\gamma_0}{\gamma_{\mathbf{g}}})} \delta(\lambda_{\mathbf{g}} - \lambda_{\mathbf{g}}^*), \tag{12b}$$

where we use the relation $\delta(\lambda_0 - \lambda_0^*) = \frac{\gamma_{\mathbf{g}}}{\gamma_0}\delta(\lambda_{\mathbf{g}} - \lambda_{\mathbf{g}}^*)$. The diffracted field behind the radiator in vacuum is as follows:

$$E_{\mathbf{g}}^{(s)vac} = E_{\mathbf{g}}^{(s)Rad} \delta(\lambda_{\mathbf{g}} + \frac{\omega\chi_0}{2}), \tag{12c}$$

where $E_{\mathbf{g}}^{(s)Rad}$ is the field of coherent radiation in the direction close to the Bragg direction. From the second equation of the system (3) we can derive the expression relating the incident and diffracted fields in the medium:

$$E_0^{(s)medium} = \frac{2\omega\lambda_{\mathbf{g}}}{\omega^2\chi_g C^{(s)}} E_{\mathbf{g}}^{(s)medium}. \tag{13}$$

To determine the amplitude of the field $E_{\mathbf{g}}^{(s)Rad}$, we use the boundary conditions at the entrance and exit surfaces of the multilayer plate:

$$\int E_0^{(s)vacI} d\lambda_0 = \int E_0^{(s)medium} d\lambda_0, \tag{14a}$$

$$\int E_{\mathbf{g}}^{(s)medium} d\lambda_0 = 0, \tag{14b}$$

$$\int E_{\mathbf{g}}^{(s)medium} exp(i\frac{\lambda_{\mathbf{g}}}{\gamma_{\mathbf{g}}}L) d\lambda_{\mathbf{g}} =$$
$$= \int E_{\mathbf{g}}^{(s)vac} exp(i\frac{\lambda_{\mathbf{g}}}{\gamma_{\mathbf{g}}}L) d\lambda_{\mathbf{g}}. \tag{14c}$$

We will present the radiation field in the form of two terms:

$$E_{\mathbf{g}}^{(s)Rad} = E_{PXR}^{(s)} + E_{DTR}^{(s)}, \tag{15a}$$

$$E_{PXR}^{(s)} = -\frac{8\pi^2 ieV\theta P^{(s)}}{\omega} \frac{\omega^2\chi_{\mathbf{g}} C^{(s)}}{8\frac{\gamma_0}{\gamma_{\mathbf{g}}}\sqrt{\beta^2 + 4\chi_{\mathbf{g}}\chi_{-\mathbf{g}}C^{(s)}\frac{\gamma_{\mathbf{g}}}{\gamma_0}}} \frac{1}{\lambda_0^*} \times \left[\left(\beta + \sqrt{\beta^2 + 4\chi_{\mathbf{g}}\chi_{-\mathbf{g}}C^{(s)}\frac{\gamma_{\mathbf{g}}}{\gamma_0}}\right) \times\right.$$
$$\times \left(\frac{1 - exp(-i\frac{\lambda_{\mathbf{g}}^* - \lambda_{\mathbf{g}}^{(2)}}{\gamma_{\mathbf{g}}}L)}{\lambda_{\mathbf{g}}^* - \lambda_{\mathbf{g}}^{(2)}}\right) - \left(\beta - \sqrt{\beta^2 + 4\chi_{\mathbf{g}}\chi_{-\mathbf{g}}C^{(s)}\frac{\gamma_{\mathbf{g}}}{\gamma_0}}\right) \times$$
$$\left.\times \left(\frac{1 - exp(-i\frac{\lambda_{\mathbf{g}}^* - \lambda_{\mathbf{g}}^{(1)}}{\gamma_{\mathbf{g}}}L)}{\lambda_{\mathbf{g}}^* - \lambda_{\mathbf{g}}^{(1)}}\right)\right] exp\left[i(\frac{\omega\chi_0}{2} + \lambda_g^*)\frac{L}{\gamma_g}\right], \tag{15b}$$

$$E_{DTR}^{(s)} = \frac{8\pi^2 ieV\theta P^{(s)}}{\omega} \frac{\chi_{\mathbf{g}} C^{(s)}}{\frac{\gamma_0}{\gamma_{\mathbf{g}}}\sqrt{\beta^2 + 4\chi_{\mathbf{g}}\chi_{-\mathbf{g}}C^{(s)}\frac{\gamma_{\mathbf{g}}}{\gamma_0}}} \left(\frac{\omega}{-\omega\chi_0 - 2\lambda_0^*} + \frac{\omega}{2\lambda_0^*}\right) \times$$
$$\times \left[exp\left(-i\frac{\lambda_{\mathbf{g}}^* - \lambda_{\mathbf{g}}^{(1)}}{\gamma_{\mathbf{g}}}L\right) - exp\left(-i\frac{\lambda_{\mathbf{g}}^* - \lambda_{\mathbf{g}}^{(2)}}{\gamma_{\mathbf{g}}}L\right)\right] exp\left[i\left(\frac{\omega\chi_0}{2} + \lambda_g^*\right)\frac{L}{\gamma_g}\right]. \tag{15c}$$

The expression (15b) and (15c) represent the amplitudes of the radiation fields, similar to the amplitudes of PXR and DTR in a crystal. The DTR is the result of diffraction by a periodically layered artificial structure of the transition radiation, which is generated on the front surface of the target. For further analysis of the radiation, the dynamic addition (9) can be represented as follows:

$$\lambda_g^{(1,2)} = \frac{\omega|\chi'_{\mathbf{g}}|C^{(s)}}{2}\Bigg(\xi^{(s)} - \frac{i\rho^{(s)}(1-\varepsilon)}{2} \pm$$

$$\pm\sqrt{{\xi^{(s)}}^2 + \varepsilon - 2i\rho^{(s)}\left(\frac{(1-\varepsilon)}{2}\xi^{(s)} + \kappa^{(s)}\varepsilon\right) - {\rho^{(s)}}^2\left(\frac{(1-\varepsilon)^2}{4} + {\kappa^{(s)}}^2\varepsilon\right)}\Bigg), \qquad (16)$$

where $\xi^{(s)} = \eta^{(s)}(\omega) + \frac{1-\varepsilon}{2\nu^{(s)}}$,

$$\eta^{(s)}(\omega) = \frac{\alpha}{2\left|Re\sqrt{\chi_{\mathbf{g}}\chi_{-\mathbf{g}}}\right|C^{(s)}} \equiv \frac{\sin^2\theta_B}{V^2C^{(s)}}\frac{gT}{|\chi'_b - \chi'_a|\left|\sin\left(\frac{ga}{2}\right)\right|}\left(1 - \frac{\omega(1-\theta\cos\varphi\cot\theta_b)}{\omega_B}\right),$$

$$\nu^{(s)} = \frac{C^{(s)}Re\sqrt{\chi_{\mathbf{g}}\chi_{-\mathbf{g}}}}{\chi'_0} \equiv \frac{2C^{(s)}\left|\sin(\frac{ga}{2})\right|}{g}\left|\frac{\chi'_b - \chi'_a}{a\chi'_a + b\chi'_b}\right|,$$

$$\rho^{(s)} = \frac{\chi''_0}{\left|Re\sqrt{\chi_{\mathbf{g}}\chi_{-\mathbf{g}}}\right|C^{(s)}} \equiv \frac{a\chi''_a + b\chi''_b}{|\chi'_b - \chi'_a|C^{(s)}}\frac{g}{2\left|\sin\left(\frac{ga}{2}\right)\right|},$$

$$\kappa^{(s)} = \frac{\chi''_{\mathbf{g}}C^{(s)}}{\chi''_0} \equiv \frac{2C^{(s)}\left|\sin\left(\frac{ga}{2}\right)\right|}{g}\left|\frac{\chi''_b - \chi''_a}{a\chi''_a + b\chi''_b}\right|, \varepsilon = \frac{\gamma_{\mathbf{g}}}{\gamma_0}. \qquad (17)$$

An important parameter in (17) is the parameter that determines the degree of the field reflection asymmetry relative to the target surface, which can be represented as

$$\varepsilon = \frac{\sin(\delta + \theta_B)}{\sin(\delta - \theta_B)}, \qquad (18)$$

where θ_B is the angle between the electron velocity and reflective layers, δ - the angle between the target surface and reflective layers. Note that the angle of electron incidence on the target surface increases when the parameter decreases, and vice versa (see Fig.2).

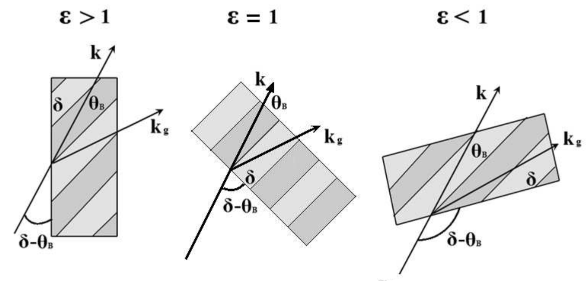

Fig.2. *Schema of the asymmetric ($\varepsilon > 1$ and $\varepsilon < 1$ cases) reflection of the radiation from the crystal plate. The case ($\varepsilon = 1$) corresponds to the symmetric reflection*

3. SPECTRAL-ANGULAR RADIATION DENSITY

Substituting (16) for $\lambda_g^{(1,2)}$ into (15b) and (15c), then substituting (15b) for $E_{PXR}^{(s)}$ and (15c) for in the well-known [19] expression for the spectral-angular density of X-rays

$$\omega\frac{d^2N}{d\omega d\Omega} = \omega^2(2\pi)^{-6}\sum_{s=1}^{2}\left|E_{\mathbf{g}}^{(s)Rad}\right|^2, \qquad (19)$$

we will obtain the expression for summands, describing the contributions to the spectral-angular density of the radiation of the mechanisms PXR, DTR and of the summand, which is the result of the interference of these radiation mechanisms.

$$\omega\frac{d^2N_{PXR}^{(s)}}{d\omega d\Omega} = \frac{e^2}{4\pi^2}P^{(s)}\frac{\theta^2}{\left(\theta^2 + \gamma^{-2} - \chi'_0\right)^2}R_{PXR}^{(s)}, \qquad (20a)$$

$$R_{PXR}^{(s)} = \frac{1 + exp(-2b^{(s)}\rho^{(s)}\Delta^{(1)}) - 2exp(-b^{(s)}\rho^{(s)}\Delta^{(1)})\cos\left(b^{(s)}\left(\sigma^{(s)} + \frac{\xi-\sqrt{\xi^2+\varepsilon}}{\varepsilon}\right)\right)}{\left(\sigma^{(s)} + \frac{\xi-\sqrt{\xi^2+\varepsilon}}{\varepsilon}\right)^2 + {\rho^{(s)}}^2{\Delta^{(1)}}^2}\times$$

$$\times\left(1 - \frac{\xi}{\sqrt{\xi^2+\varepsilon}}\right)^2 \qquad (20b)$$

$$\omega\frac{d^2N_{DTR}^{(s)}}{d\omega d\Omega}=\frac{e^2}{4\pi^2}P^{(s)2}\theta^2\left(\frac{1}{\theta^2+\gamma^{-2}}-\frac{1}{\theta^2+\gamma^{-2}-\chi_0'}\right)^2R_{DTR}^{(s)}, \tag{21a}$$

$$R_{DTR}^{(s)}=\frac{4\varepsilon^2}{\xi^2+\varepsilon}exp\left(-b^{(s)}\rho^{(s)}\frac{1+\varepsilon}{\varepsilon}\right)\times\left[\sin^2\left(b^{(s)}\frac{\left(\sqrt{\xi^2+\varepsilon}\right)}{\varepsilon}\right)+sh^2\left(b^{(s)}\rho^{(s)}\frac{(1-\varepsilon)\xi^{(s)}+2\varepsilon\kappa^{(s)}}{2\varepsilon\sqrt{\xi^2+\varepsilon}}\right)\right], \tag{21b}$$

where

$$\Delta^{(1)}=\frac{\varepsilon+1}{2\varepsilon}-\frac{1-\varepsilon}{2\varepsilon}\frac{\xi^{(s)}}{\sqrt{\xi^{(s)2}+\varepsilon}}-\frac{\kappa^{(s)}}{\sqrt{\xi^{(s)2}+\varepsilon}},$$

$$\sigma^{(s)}=\frac{1}{|\chi_{\mathbf{g}}'|C^{(s)}}(\theta^2+\gamma^{-2}-\chi_0')\equiv\frac{1}{\nu^{(s)}}\left(\frac{\theta^2}{|\chi_0'|}+\frac{1}{\gamma^2|\chi_0'|}+1\right),$$

$$b^{(s)}=\frac{\omega|Re\sqrt{\chi_{\mathbf{g}}\chi_{-\mathbf{g}}}|C^{(s)}}{2}\frac{L}{\gamma_0}. \tag{22}$$

The expressions (20)-(21) constitute the main result of this work. They are obtained in two-wave approximation of dynamic diffraction theory, taking into account the absorption of radiation in the layered plate substances and the orientation of the diffracting layers relative to the surface of the plate. These expressions allow us to investigate the spectral and angular characteristics of radiation depending on the energy of relativistic electrons and on the parameters of the artificial periodic structure of the target.

4. ANALYSIS OF DTR WAVE. BORMANN EFFECT

Since two X-ray waves determine the DTR yield, for the analysis of their contributions to the radiation spectral density it is convenient to represent the expression (21b) in such a form:

$$R_{DTR}^{(s)}=\frac{\varepsilon^2}{\xi(\omega)^2+\varepsilon}\left[e^{-b^{(s)}\rho^{(s)}\left(\frac{1+\varepsilon}{\varepsilon}-\frac{(1-\varepsilon)\xi^{(s)}+2\varepsilon\kappa^{(s)}}{\varepsilon\sqrt{\xi^2+\varepsilon}}\right)}+e^{-b^{(s)}\rho^{(s)}\left(\frac{1+\varepsilon}{\varepsilon}+\frac{(1-\varepsilon)\xi^{(s)}+2\varepsilon\kappa^{(s)}}{\varepsilon\sqrt{\xi^2+\varepsilon}}\right)}-\right.$$

$$\left.-2\cdot e^{-b^{(s)}\rho^{(s)}\frac{1+\varepsilon}{\varepsilon}}\cdot\cos\left(\frac{2b^{(s)}\sqrt{\xi^2+\varepsilon}}{\varepsilon}\right)\right]. \tag{23}$$

When consider the expression (23), one can see that the terms in brackets successively describe the waves belonging to the first and second fields, and their interference. Next we write the expression (23) in a more demonstrable form of

$$R_{DTR}^{(s)}=\frac{\varepsilon^2}{\xi(\omega)^2+\varepsilon}\left[e^{-L_f\mu_1^{(s)}}+e^{-L_f\mu_2^{(s)}}-2\cdot e^{-L_f\mu_0\left(\frac{1+\varepsilon}{2}\right)}\cdot\cos\left(\frac{L_f}{L_{ext}^{(s)}}\sqrt{\xi^2+\varepsilon}\right)\right], \tag{24}$$

where

$$\mu_1^{(s)}=\mu_0\left[\frac{1+\varepsilon}{2}-\frac{(1-\varepsilon)\xi^{(s)}+2\varepsilon\kappa^{(s)}}{2\sqrt{\xi^2+\varepsilon}}\right],$$

$$\mu_2^{(s)}=\mu_0\left[\frac{1+\varepsilon}{2}+\frac{(1-\varepsilon)\xi^{(s)}+2\varepsilon\kappa^{(s)}}{2\sqrt{\xi^2+\varepsilon}}\right], \tag{25}$$

where L_f is the path of a photon in a crystal, $\mu_0=\omega\chi_0''$- the linear coefficient of X-waves absorption in the averaged amorphous medium, $L_{ext}^{(s)}=\frac{1}{\omega|Re\sqrt{\chi_{\mathbf{g}}\chi_{-\mathbf{g}}}|C^s}$ - the length of the X-waves extinction in a periodic medium. The formula (24) clearly demonstrates the dynamic Borrmann effect arising during the passage of X-rays DTR through a periodic medium. Namely, in the X-ray scattering in a periodical medium the abnormal weak absorption is observed for the first wave field $\mu_1^{(s)}\ll\mu_0$ (i.e. anomalous transmission of the first field X-rays) and abnormal strong absorption for the second one $\mu_2^{(s)}>\mu_0$. By this reason, for the sufficiently large photon path in the substance of the plate the DTR only by one of the fields in a periodic structure will be formed, namely, by the field with effective absorption coefficient $\mu_1^{(s)}$.

Physics of the Borrmann effect [20] consists in the formation of the standing waves from the incident and scattered waves, whose antinodes are localized in the regions of space with a lower electron density for one of the waves (first term in (23) and (24)) and in the regions of space with a higher electron density for second wave (second term in (23) and (24)). Parameter $\kappa^{(s)}$ appearing in (25) determines the degree of manifestation of the Borrmann effect in the anomalous X-ray waves passing through a periodic structure. As in the case of free X-ray waves in crystals, a prerequisite for manifestation of the effect of DTR in layered medium is the condition $\kappa^{(s)} \approx 1$, corresponds to the minimal value of the linear absorption coefficient $\mu_1^{(s)}$. Next, we will carry out a numerical analysis for each of the waves and of their interference term separately. For this purpose the expression (23) we write in the following form

$$R_{DTR}^{(s)} = R_1^{(s)} + R_2^{(s)} + R_{int}^{(s)}, \qquad (26a)$$

$$R_1^{(s)} = \frac{\varepsilon^2}{\xi(\omega)^2 + \varepsilon} e^{-b^{(s)}\rho^{(s)}\left(\frac{1+\varepsilon}{\varepsilon} - \frac{(1-\varepsilon)\xi^{(s)}+2\varepsilon\kappa^{(s)}}{\varepsilon\sqrt{\xi^2+\varepsilon}}\right)}, \qquad (26b)$$

$$R_2^{(s)} = \frac{\varepsilon^2}{\xi(\omega)^2 + \varepsilon} e^{-b^{(s)}\rho^{(s)}\left(\frac{1+\varepsilon}{\varepsilon} + \frac{(1-\varepsilon)\xi^{(s)}+2\varepsilon\kappa^{(s)}}{\varepsilon\sqrt{\xi^2+\varepsilon}}\right)}, \qquad (26c)$$

$$R_{int}^{(s)} = -\frac{2\varepsilon^2}{\xi(\omega)^2 + \varepsilon} e^{-b^{(s)}\rho^{(s)}\frac{1+\varepsilon}{\varepsilon}} \cdot \cos\left(\frac{2b^{(s)}\sqrt{\xi^2+\varepsilon}}{\varepsilon}\right) \qquad (26d)$$

We will carry out the calculations for σ-polarized waves, i.e. for $s = 1$. In order to get demonstrable results, we will consider the case when the layers are of equal thickness $a = b = T/2$. We will consider the reflections, that correspond to $g = \frac{2\pi}{T}$. In this case, the parameters in the expressions (26) will take the following values:

$$\xi(\omega) = \frac{2\pi\sin^2(\theta_B)}{|\chi_b' - \chi_a'|} \cdot \left(1 - \frac{\omega}{\omega_B}\right) + \frac{1-\varepsilon}{2\nu^{(1)}},$$

$$\kappa^{(1)} = \frac{2}{\pi} \cdot \left|\frac{\chi_b'' - \chi_a''}{\chi_b' + \chi_a'}\right|, \rho^{(1)} = \frac{\pi}{2} \cdot \left|\frac{\chi_b'' + \chi_a''}{\chi_b' - \chi_a'}\right|,$$

$$\nu^{(1)} = \frac{2}{\pi} \cdot \left|\frac{\chi_b' - \chi_a'}{\chi_b' + \chi_a'}\right|, b^{(1)} = \frac{\omega_B|\chi_b' - \chi_a'|}{2\pi\sin(\delta - \theta_B)} L. \qquad (27)$$

For a thin target ($b^{(1)} = 5$), the curves drawn by (26), are s hown in Fig. 3 describing the spectral density of the DTR (for $\omega_B = 8\kappa eV$) in the artificial periodic structure consisting of amorphous layers of beryllium (Be) and tungsten (W). We see in this case, that the DTR is formed by the fields of two waves in a periodic structure, whose contributions in the spectral distribution are of comparable magnitude which will cause a strong interference of these waves. The interference term brings oscillations in the spectral density.

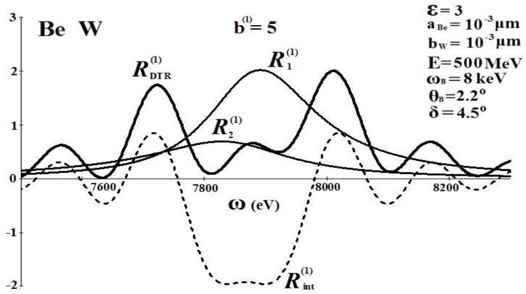

Fig.3. *The contributions of the two fields, $R_1^{(1)}$ and $R_2^{(1)}$, and of their interference term $R_{int}^{(1)}$ into the total spectral density of DTR $R_{DTR}^{(1)} = R_1^{(1)} + R_2^{(1)} + R_{int}^{(1)}$*

With increase of the target thickness one of the waves decays rapidly (Figs. 4, 5), while the other one traverses the target without a significant decrease in amplitude. Under these conditions the contribution of the interference term markedly decreases and the spurious peaks in the spectrum are attenuated and then completely disappear (Fig. 6).

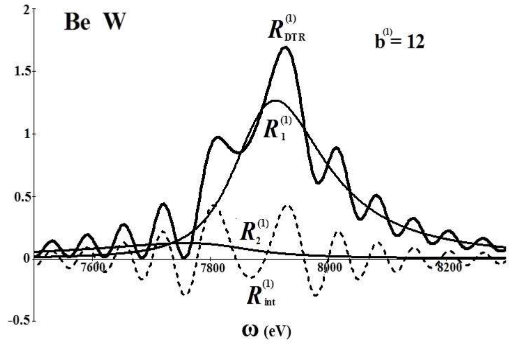

Fig.4. *The same as Fig.3 for bigger target thickness*

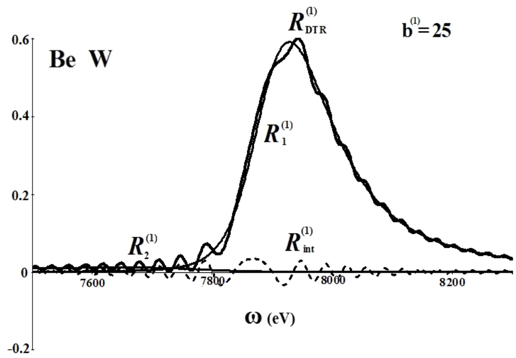

Fig.5. *The same as in Fig.4 for bigger target thickness*

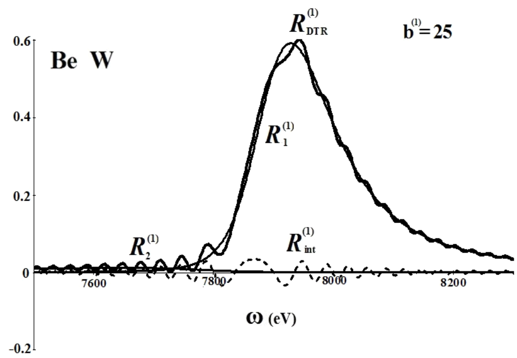

Fig.6. *The spectral density of the relativistic electron DTR for different values of the target thickness*

It should be noted that the spectral curves in Fig. 5 and Fig. 6 are constructed for a large target thickness, when the photon path length is longer than the average photo-absorption in an amorphous medium $l_{abs} = \frac{1}{\mu_0}$, which corresponds to the conditions of the Borrmann effect manifestation in an artificial periodic structure. We should note also that with the increase in target thickness the monochromaticity of DTR grows.

5. ANGULAR DENSITY OF DTR AND PXR

For the case of σ- polarized waves the expressions (20) and (21) describing the spectral-angular distributions of PXR and DTR take the form:

$$\omega\frac{d^2N^{(1)}_{PXR}}{d\omega d\Omega}=\frac{e^2}{4\pi^2}\frac{\theta_\perp^2}{\left(\theta_\perp^2+\gamma^{-2}+\frac{|\chi'_a+\chi'_b|}{2}\right)^2}R_{PXR}, \tag{27a}$$

$$R_{PXR}=\left(1-\frac{\xi(\omega)}{\sqrt{\xi(\omega)^2+\varepsilon}}\right)^2\frac{1+e^{-2b^{(1)}\rho^{(1)}\Delta^{(1)}}-2e^{-b^{(1)}\rho^{(1)}\Delta^{(1)}}\cos\left(b^{(1)}\Omega^{(1)}(\omega)\right)}{\Omega^{(1)}(\omega)^2+\left(\rho^{(s)}\Delta^{(1)}\right)^2}, \tag{27b}$$

$$\omega\frac{d^2N^{(1)}_{PXR}}{d\omega d\Omega}=\frac{e^2}{4\pi^2}\theta_\perp^2\left(\frac{1}{\theta_\perp^2+\gamma^{-2}}-\frac{1}{\theta_\perp^2+\gamma^{-2}+\frac{|\chi'_a+\chi'_b|}{2}}\right)^2R_{DTR}, \tag{28a}$$

$$R_{DTR}=\frac{4\varepsilon^2}{\xi(\omega)^2+\varepsilon}exp\left(-b^{(1)}\rho^{(1)}\frac{1+\varepsilon}{\varepsilon}\right)\times$$
$$\times\left[\sin^2\left(b^{(1)}\frac{\left(\sqrt{\xi(\omega)^2+\varepsilon}\right)}{\varepsilon}\right)+sh^2\left(b^{(1)}\rho^{(1)}\frac{(1-\varepsilon)\xi(\omega)+2\varepsilon\kappa^{(1)}}{2\varepsilon\sqrt{\xi(\omega)^2+\varepsilon}}\right)\right], \tag{28b}$$

where

$$\Omega^{(1)}(\omega)=\sigma(\theta,\gamma)+\left(\xi(\omega)-\sqrt{\xi(\omega)^2+\varepsilon}\right)/\varepsilon,$$

$$\sigma(\theta,\gamma)=\frac{\pi}{|\chi'_b-\chi'_a|}\left(\theta_\perp^2+\gamma^{-2}+\frac{|\chi'_a+\chi'_b|}{2}\right)$$

$$\Delta^{(1)}=\frac{1+\varepsilon}{2\varepsilon}-\frac{1-\varepsilon}{2\varepsilon}\frac{\xi}{\sqrt{\xi^2+\varepsilon}}-\frac{\kappa^{(1)}}{\sqrt{\xi^2+\varepsilon}},$$

$$\xi(\omega)=\frac{2\pi\sin^2(\theta_B)}{|\chi'_b-\chi'_a|}\cdot(1-\frac{\omega}{\omega_B})+\frac{1-\varepsilon}{2\nu^{(1)}},$$

$$\kappa^{(1)}=\frac{2}{\pi}\cdot\left|\frac{\chi''_b-\chi''_a}{\chi''_b+\chi''_a}\right|$$

$$\rho^{(1)}=\frac{\pi}{2}\cdot\left|\frac{\chi''_b+\chi''_a}{\chi''_b-\chi''_a}\right|$$

$$\nu^{(1)}=\frac{2}{\pi}\cdot\left|\frac{\chi'_b-\chi'_a}{\chi'_b+\chi'_a}\right|$$

$$b^{(1)}=\frac{\omega_B|\chi'_b-\chi'_a|}{2\pi sin(\delta-\theta_B)}L,\theta_\perp=\theta\sin\varphi. \tag{29}$$

The angular densities of PXR and DTR of relativistic electron in periodical multilayer plate can be written in the following way:

$$\frac{dN^{(1)}_{PXR}}{d\Omega}=\frac{e^2}{4\pi^2}\frac{\theta_\perp^2}{\left(\theta_\perp^2+\gamma^{-2}+\frac{|\chi'_a+\chi'_b|}{2}\right)^2}\int R_{PXR}\frac{d\omega}{\omega}, \tag{30a}$$

$$\frac{dN^{(1)}_{DTR}}{d\Omega}=\frac{e^2}{4\pi^2}\theta_\perp^2\left(\frac{1}{\theta_\perp^2+\gamma^{-2}}-\frac{1}{\theta_\perp^2+\gamma^{-2}+\frac{|\chi'_a+\chi'_b|}{2}}\right)^2\int R_{DTR}\frac{d\omega}{\omega}. \tag{30b}$$

To bring into comparison the angular radiation densities in artificial periodic and crystal media in approximately equal conditions, we write the expression for the angular density of DTR in the crystal for - polarized waves in the following way:

$$\frac{dN^{(1)Cr}_{DTR}}{d\Omega}=\frac{e^2}{4\pi^2}\theta_\perp^2\left(\frac{1}{\theta_\perp^2+\gamma^{-2}}-\frac{1}{\theta_\perp^2+\gamma^{-2}-\chi'_0}\right)^2\int R_{DTR}\frac{d\omega}{\omega}. \tag{31}$$

Here the notations corresponding to (26) have the form

$$\kappa^{(1)}=\frac{\chi''_{\mathbf{g}}}{\chi''_0},\rho^{(1)}=\frac{\chi''_0}{|\chi'_{\mathbf{g}}|},\nu^{(1)}=\frac{\chi'_{\mathbf{g}}}{\chi'_0},\sigma(\theta,\gamma)=\frac{1}{|\chi'_{\mathbf{g}}|}\cdot(\theta_\perp^2+\gamma^{-2}-\chi'_0),$$

$$\xi(\omega)=\frac{2\sin^2(\theta_B)}{|\chi'_{\mathbf{g}}|}\cdot(1-\frac{\omega}{\omega_B})+\frac{1-\varepsilon}{2\nu^{(1)}},\theta_\perp=\theta\sin\varphi. \tag{32}$$

By formulae (30 b) and (31) the curves of the angular density of DTR ($\omega_B = 8\kappa eV$) in the crystalline tungsten (W) target (see Fig. 7) and DTR in an artificial periodic structure consisting of amorphous layers of beryllium Be and tungsten W (Fig. 8) are constructed.

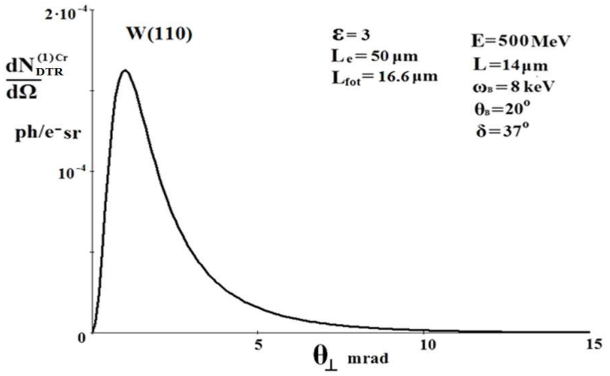

Fig.7. The angular density of DTR of the relativistic electron crossing a plate of single crystal (W)

The paths of the electron $L_e = 50\mu m$ and of DTR photon $L_{fot} = 16,6\mu m$ in the target have been chosen the same for both the cases. As it follows from Fig. 7 and Fig. 8 the angular density of the DTR in the artificial periodic structure is more than three orders of magnitude greater than the angular density of the crystal DTR in the crystal under similar conditions.

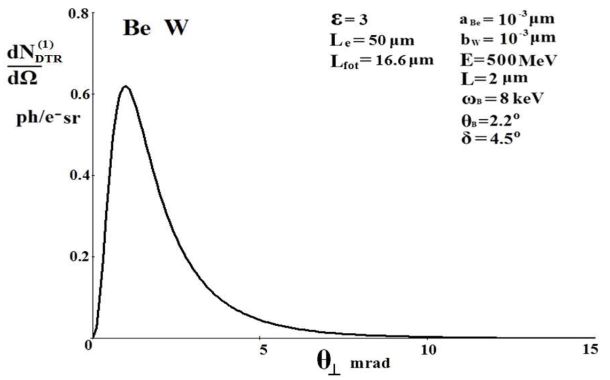

Fig.8. The DTR angular density of the relativistic electron crossing the artificial periodic structure (Be W) under the conditions close to the ones which presented in Fig.7

The curves in Fig. 9, constructed by the formula (27) demonstrate the DTR spectra in the artificial periodic structure for different observation angles. As it follows from Fig. 9, the frequency of the DTR considerably depends on the observation angle that leads to the radiation monochromaticity degradation. Curves in Fig. 10, constructed by the formula (28), show the spectra of DTR at two different angles of the observation. It follows from Fig. 10, that DTR is more monochromatic than PXR, which is interesting from the standpoint of creating an intense quasi-monochromatic X-ray source. It should be noted that the curves in Fig. 10, as in Fig. 8 are built under the conditions when the Bormann effect is pronounced in artificial periodic structure.

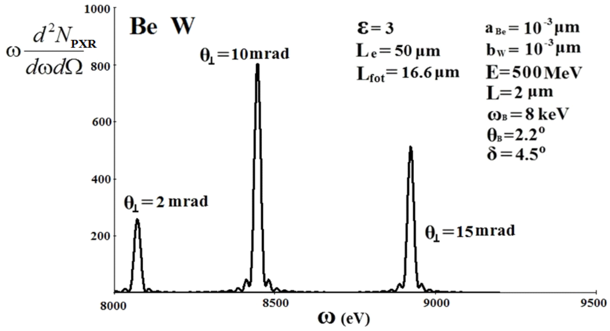

Fig.9. The spectra of the PXR at different observation angles

Let us consider the effect of reflection asymmetry in the field relative to the target surface on the spectral-angular characteristics of the DTR.

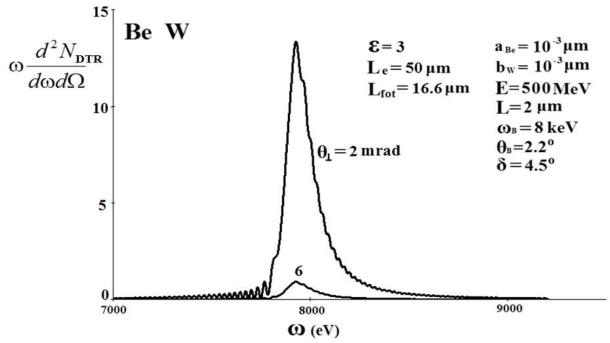

Fig.10. The spectra of the DTR at different observation angles

Figs. 11 and 12 show curves similar to curves constructed in Figs. 8 and 10, but for the other value of the asymmetry parameter ε. The length of the photon path $L_{fot} = 16,6\mu m$ is taken the same in both the cases. We can see that the width of the DTR spectrum increases with the increase of asymmetry (see Fig. 12), which leads to an increase in the angular density of DTR (11). This effect is due to the dependence of the linear absorption coefficient of the first field (25) on the asymmetry of reflection.

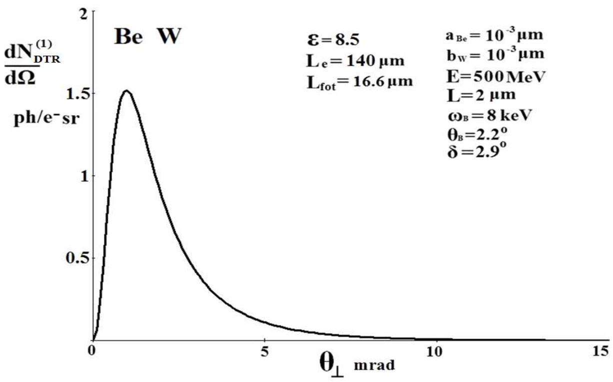

Fig.11. The same as in Fig.8 under other value of asymmetry parameter ε

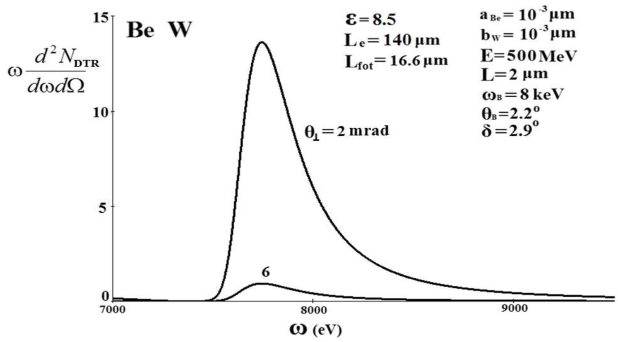

Fig.12. *The same as in Fig.10, but for other value of asymmetry parameter ε*

Let us consider the opportunity to optimize the DTR yield, choosing a target thickness value L. For this we construct the dependence on the target thickness of the angular density of DTRI at a fixed angle of observation (Fig. 13). As it is seen in Fig. 13, when the target thickness increases the density of PDI at first increases but then decreases because of absorption in medium.

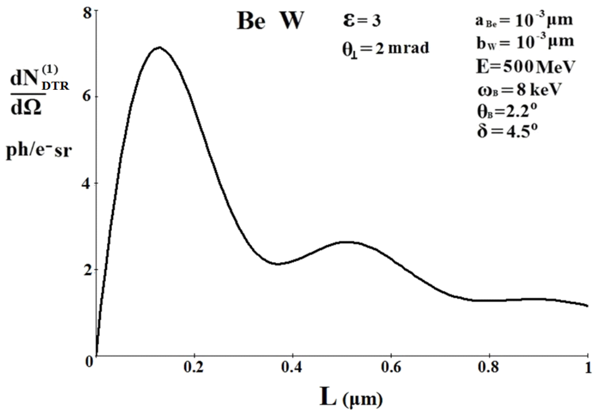

Fig.13. *The dependence of the DTR yield on the target thickness for a fixed observation angle θ*

The oscillations observed in the dependence of the radiation angular density on target thickness reflects the process of energy transfer from the incident wave to reflected wave and back. The target thickness corresponding to the first maximum in the curve of the DTR angular density is optimal for the target as a radiator. We present the calculated curves for the angular density of DTR and PXR at the optimum target thickness in Fig. 13. As it seen from Fig. 14, the angular density of DTR is significantly higher than the angular density of PXR in the same target and more than 10 times higher than the angular density for the DTR in a target of nonoptimal thickness shown in Fig. 8.

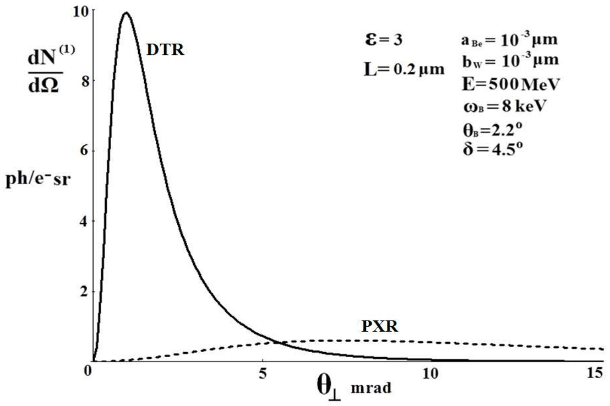

Fig.14. *The comparison of the DTR and PXR densities for optimal for DTR thickness of the target*

6. CONCLUSIONS

A theory for the coherent radiation of the relativistic electron crossing an artificial periodic structure is constructed for the case of Laue scattering geometry. The expressions for spectral-angular characteristics of the radiation in Bragg direction are derived and investigated.

The contributions to the DTR yield of two X-ray waves, which are responsible for DTR formation, are studied. It is shown that with increase of the target thickness, one of the waves is absorbed anomalously strongly and the other wave abnormally weakly, i.e. the Borrmann effect is manifested in DTR in an artificial periodic structure in the Laue geometry

Based on these expression it is shown that the angular density of diffracted transition radiation in layered target is more than one order higher than the density for a single crystal radiator under similar conditions.

It was found, that DTR in artificial periodic structure is more monochromatic than parametric X-radiation (PXR). In this connection, DTR mechanism may be more promising in terms of the building a new intense tunable X-ray source on the basis of the relativistic electron interaction with artificial multilayer structure. It is shown, that DTR yield in an artificial periodic structure in the direction of maximum angular density is increasing as a function of target thickness up to some optimal value of thickness and then decrease because of the photoabsorption in the target substance.

References

1. G.M. Garibian, C. Yang. *X- ray Transition Radiation.* Erevan, 1983 (in Russian).

2. A. Caticha // *Phys. Rev. A.* 1989, v. 40, p. 4322.

3. N.N. Nasonov // *Phys. Lett. A.* 1998, v. 246, p. 148.

4. X. Artru, P. Rullhusen // *Nucl. Instr. Meth. B.*

1998, v. 145, p. 1.

5. M. Ter-Mikaelian. *High-Energy Electromagnetic Process in Condensed Media.* 1972, New York: "Wiley".

6. G. Garibian, C. Yang // *J. Exp. Theor. Phys.* 1971, v.61, p.930.

7. V. Baryshevsky, I. Feranchuk // *J. Exp. Theor. Phys.* 1971, v. 61, p. 944.

8. N. Nasonov, V. Noskov // *Nucl. Instr. Meth. B.* 2003, v. 201, p. 67.

9. A.S. Kubankin, N.N. Nasonov, V.I. Sergienko, I.E. Vnukov // *Nucl. Instr. Meth. B.* 2003, v. 201, p. 97.

10. Y.N. Adischev, S.N. Arishev, A.V. Vnukov, et al. // *Nucl. Instr. Meth. B.* 2003, v. 201. p. 114.

11. N.N. Nasonov, V.V. Kaplin, S.R. Uglov, et al. // *Nucl. Instr. Meth. B.* 2005, v. 227. p. 41.

12. S. Blazhevich, A. Noskov // *Nucl. Instr. Meth. B.* 2006. v. 252. p. 69.

13. S.V. Blazhevich, A.V. Noskov // *Nucl. Instr. Meth. B.* 2008, v. 266. p. 3777.

14. S. Blazhevich, A.J. Noskov // *Exp. Theor. Phys.* 2009, v. 136, p. 1043.

15. S.V. Blazhevich, A.V. Noskov // *Nucl. Instr. Meth. B.* 2008, v. 266. p. 3770.

16. M.A. Piestrup, D.G. Boyers, C.I. Pincus, et al. // *Phys.Rev. A.* 1992, v. 45. p. 1183.

17. N.N. Nasonov, V.V. Kaplin, S.R. Uglov, M.A. Piestrup, C.K. Gary // *Phys. Rev. E.* 2003, v. 68. p. 3604.

18. Z. Pinsker. *Dynamic Scattering of X-rays in Crystals*, Berlin: "Springer", 1984.

19. V. Bazylev, N. Zhevago. *Emission From Fast Particles Moving in a Medium and External Fields.* Moscow: "Nauka", 1987.

20. G. Borrmann. // *Zh. Phys.* 1941, v. 42. p. 157.

ДИНАМИЧЕСКАЯ ТЕОРИЯ ИЗЛУЧЕНИЯ РЕЛЯТИВИСТСКОГО ЭЛЕКТРОНА В ПЕРИОДИЧЕСКОЙ СЛОИСТОЙ СРЕДЕ В ГЕОМЕТРИИ ЛАУЭ

С.В. Блажевич, Ю.П. Гладких, А.В. Носков

Построена теория когерентного рентгеновского излучения релятивистского электрона, пересекающего искусственную периодическую среду в геометрии рассеяния Лауэ. Получены и исследованы выражения, описывающие спектрально-угловые характеристики излучения в направлении рассеяния Брэгга. Излучение рассматривается, по аналогии с излучением в кристаллической среде, как результат когерентного сложения вкладов двух механизмов излучения – параметрического рентгеновского (ПРИ) и дифрагированного переходного (ДПИ). Показано, что выход ДПИ из слоистой мишени может более чем на порядок превышать выход излучения частицы в монокристаллическом радиаторе в аналогичных условиях. Показаны проявления эффекта Бормана в ДПИ в периодической слоистой среде для геометрии рассеяния Лауэ.

ДИНАМІЧНА ТЕОРІЯ ВИПРОМІНЮВАННЯ РЕЛЯТИВІСТСЬКОГО ЕЛЕКТРОНА В ПЕРІОДИЧНОМУ ШАРОВОМУ СЕРЕДОВИЩІ В ГЕОМЕТРІЇ ЛАУЕ

С.В. Блажевич, Ю.П. Гладких, А.В. Носков

Побудована теорія когерентного рентгенівського випромінювання релятивістського електрона, який перетинає штучне періодичне середовище в геометрії розсіювання Лауе. Отримані і досліджені вирази, які описують спектрально-кутові характеристики випромінювання в напрямі розсіювання Брегга. Випромінювання розглядається, по аналогії з випромінюванням в кристалічному середовищі, як наслідок когерентної суми вкладів двох механизмів випромінювання – параметрического рентгенівського (ПРВ) та дифрагованого перехідного (ДПВ). Показано, що вихід ДПВ із шарової мішені може більше ніж на порядок перевищувати вихід випромінювання часток в монокристалічному радіаторі в аналогічних умовах. Показано винекнення эфекта Бормана в ДПВ в періодичному шаровому середовищі для геометрії розсіювання Лауе.